Embedded biomimetic nanostructures for enhanced optical absorption in thin-film solar cells

Min-An Tsai,[2] Hao-Wei Han,[4] Yu-Lin Tsai,[1] Ping-Chen Tseng,[1] Peichen Yu,[1,5] Hao-Chung Kuo,[1,6] Chang-Hong Shen,[3] Jia-Min Shieh,[1,3] and Shiuan-Huei Lin[2]

[1]Department of Photonics and Institute of Electro-Optical Engineering, National Chiao Tung University, Hsinchu 30010, Taiwan
[2]Department of Electro-physics, National Chiao Tung University, Hsinchu 30010, Taiwan
[3]National Nano Device Laboratories, No. 26, Prosperity Road 1, Hsinchu 30078, Taiwan
[4]Institute of Photonic System, National Chiao Tung University, Tainan 711, Taiwan
[5]yup@faculty.nctu.edu.tw
[6]hckuo@faculty.nctu.edu.tw

Abstract: Light-management is critical to thin film solar cells due to their usually limited optical absorption in the active layer. Conventional approaches involve employing separate techniques for anti-reflection and light trapping. Here, we demonstrate an embedded biomimetic nanostructure (EBN) that achieves both effects for hydrogenated amorphous silicon (a-Si:H) solar cells. The fabrication of EBNs is accomplished by patterning an index-matching silicon-nitride layer deposited on a glass substrate using polystyrene nanospheres lithography, followed by reactive ion etching. The profile of EBN is then reproduced layer by layer during the deposition of a-Si:H cells. We show that a solar cell with an optimized EBN exhibits a broadband enhanced external quantum efficiency due to both anti-reflection and light-trapping, with respect to an industrial standard cell using an Asahi U glass substrate which is mostly optimized for light trapping. Overall, the cell with an optimized EBN achieves a large short-circuit current density of 17.74 mA/cm^2, corresponding to a 37.63% enhancement over a flat control cell. The power conversion efficiency is also increased from 5.36% to 8.32%. Moreover, the light management enabled by the EBN remains efficient over a wide range of incident angles up to 60°, which is particularly desirable for real environments with diffused sun light. The novel patterning method is not restricted to a-Si:H solar cells, but is also widely applicable to other thin film materials.

OCIS codes: (310.6628) Subwavelength structures, nanostructures; (040.5350) Photovoltaic.

References and links

1. R. E. I. Schropp, and M. Zeman, *Amorphous and Microcrystalline Silicon Solar Cells: Modeling, Materials, and Device Technology* (Kluwer Academic Publishers, 1998).
2. D. E. Carlson, and C. R. Wronski, "Amorphous silicon solar cell," Appl. Phys. Lett. **28**(11), 671–673 (1976).
3. R. C. Chittick, J. H. Alexander, and H. F. Sterling, "The preparation and properties of amorphous silicon," J. Electrochem. Soc. **116**(1), 77–81 (1969).
4. A. V. Shah, H. Schade, M. Vanecek, J. Meier, E. Vallat-Sauvain, N. Wyrsch, U. Kroll, C. Droz, and J. Bailat, "Thin-film Silicon Solar Cell Technology," Prog. Photovolt. Res. Appl. **12**(23), 113–142 (2004).
5. R. E. I. Schropp, and M. Zeman, "*Amorphous and Microcrystalline Silicon Solar Cells: Modeling, Materials, and Device Technology* (Kluwer Academic Publishers, 1998).
6. J. Zhu, Z. Yu, G. F. Burkhard, C. M. Hsu, S. T. Connor, Y. Xu, Q. Wang, M. McGehee, S. Fan, and Y. Cui, "Optical absorption enhancement in amorphous silicon nanowire and nanocone arrays," Nano Lett. **9**(1), 279–282 (2009).
7. J. G. Mutitu, S. Shi, C. Chen, T. Creazzo, A. Barnett, C. Honsberg, and D. W. Prather, "Thin film solar cell design based on photonic crystal and diffractive grating structures," Opt. Express **16**(19), 15238–15248 (2008).
8. Ü. Dagkaldiran, A. Gordijn, F. Finger, H. M. Yates, P. Evans, D. W. Sheel, Z. Remes, and M. Vanecek, "Amorphous silicon solar cells made with SnO2:F TCO films deposited by atmospheric pressure CVD," Mater.

#145683 - $15.00 USD Received 11 Apr 2011; accepted 14 May 2011; published 9 Jun 2011

Sci. Eng. B **6**, 159 (2009).
9. S. Fahr, C. Rockstuhl, and F. Lederer, "Engineering the randomness for enhanced absorption in solar cells," Appl. Phys. Lett. **92**(17), 171114 (2008).
10. J. Zhu, C. M. Hsu, Z. Yu, S. Fan, and Y. Cui, "Nanodome solar cells with efficient light management and self-cleaning," Nano Lett. **10**(6), 1979–1984 (2010).
11. D. G. Stavenga, S. Foletti, G. Palasantzas, and K. Arikawa, "Light on the moth-eye corneal nipple array of butterflies," Proc. Biol. Sci. **273**(1587), 661–667 (2006).
12. A. R. Parker, and H. E. Townley, "Biomimetics of photonic nanostructures," Nat. Nanotechnol. **2**(6), 347–353 (2007).
13. Y. F. Huang, S. Chattopadhyay, Y. J. Jen, C. Y. Peng, T. A. Liu, Y. K. Hsu, C. L. Pan, H. C. Lo, C. H. Hsu, Y. H. Chang, C. S. Lee, K. H. Chen, and L. C. Chen, "Improved broadband and quasi-omnidirectional anti-reflection properties with biomimetic silicon nanostructures," Nat. Nanotechnol. **2**(12), 770–774 (2007).
14. H. Sai, Y. Kanamori, K. Arafune, Y. Ohshita, and M. Yamaguchi, "Light trapping effect of submicron surface textures in crystalline Si solar cells," Prog. Photovolt. Res. Appl. **15**(5), 415–423 (2007).
15. C. H. Chiu, P. Yu, H. C. Kuo, C. C. Chen, T. C. Lu, S. C. Wang, S. H. Hsu, Y. J. Cheng, and Y. C. Chang, "Broadband and omnidirectional antireflection employing disordered GaN nanopillars," Opt. Express **16**(12), 8748–8754 (2008).
16. Y. Kanamori, M. Sasaki, and K. Hane, "Broadband antireflection gratings fabricated upon silicon substrates," Opt. Lett. **24**(20), 1422–1424 (1999).
17. Y.-J. Lee, D. S. Ruby, D. W. Peters, B. B. McKenzie, and J. W. P. Hsu, "ZnO nanostructures as efficient antireflection layers in solar cells," Nano Lett. **8**(5), 1501–1505 (2008).
18. M.-Y. Chiu, C.-H. Chang, M.-A. Tsai, F.-Y. Chang, and P. Yu, "Improved optical transmission and current matching of a triple-junction solar cell utilizing sub-wavelength structures," Opt. Express **18**(Suppl 3), A308–A313 (2010).
19. M. A. Tsai, P. Yu, C. H. Chiu, H. C. Kuo, T. C. Lu, and S. H. Lin, "Self-assembled two-dimensional surface structures for beam shaping of GaN-based vertical-injection light-emitting diodes," IEEE Photon. Technol. Lett. **22**(1), 12–14 (2010).
20. C. H. Chiu, P. Yu, H. C. Kuo, C. C. Chen, T. C. Lu, S. C. Wang, S. H. Hsu, Y. J. Cheng, and Y. C. Chang, "Broadband and omnidirectional antireflection employing disordered GaN nanopillars," Opt. Express **16**(12), 8748–8754 (2008).
21. M. A. Tsai, P. C. Tseng, H. C. Chen, H. C. Kuo, and P. Yu, "Enhanced conversion efficiency of a crystalline silicon solar cell with frustum nanorod arrays," Opt. Express **19**(Suppl 1), A28–A34 (2011).
22. Y. K. Ee, R. A. Arif, N. Tansu, P. Kumnorkaew, and J. F. Gilchrist, Enhancement of light extraction efficiency of InGaN quantum wells light emitting diodes using SiO_2/polystyrene microlens arrays," Appl. Phys. Lett. **91**(22), 221107 (2007).
23. Y. K. Ee, R. A. Arif, H. Tong, H. P. Zhao, J. F. Gilchrist, and N. Tansu, "Optimization of light extraction efficiency of III-nitride LEDs with self-assembled colloidal-based microlenses," IEEE J. Sel. Top. Quantum Electron. **15**(4), 1218–1225 (2009).
24. Y. K. Ee, P. Kumnorkaew, R. A. Arif, H. Tong, J. F. Gilchrist, and N. Tansu, "Light extraction efficiency enhancement of InGaN quantum wells light-emitting diodes with polydimethylsiloxane concave microstructures," Opt. Express **17**(16), 13747–13757 (2009).
25. W. Ley, E. Plescher, A. Freiburg, N. Nikolaizig, and A. Popvitch, "SUN Simulator Calibration Procedure," in Proceedings of the Third International Symposium: Environmental Testing for Space Programmes (1997) , pp. 339–344.
26. L. Raniero, I. Ferreira, A. Pimentel, A. Goncalves, P. Canhola, E. Fortunato, and R. Martins, "Role of hydrogen plasma on electrical and optical properties of ZGO, ITO and IZO transparent and conductive coatings," Thin Solid Films **511–512**, 295–298 (2006).
27. P. C. Tseng, H. C. Chen, M. A. Tsai, C.-H. Chang, H. C. Kuo, and P. Yu, "Angle-resolved characteristics of silicon photovoltaics with passivated conical-frustum nanostructures," Sol. Energy Mater. Sol. Cells (to be published).

1. Introduction

Hydrogenated amorphous silicon (a-Si:H) based thin film solar cells are attractive candidates for large-scale photovoltaics due to their materials being highly abundant on earth and their compatibility for roll-to-roll processing [1–3]. A typical film thickness of approximately 1 μm is required for effective light absorption in the a-Si:H active layers. However, the minority carrier diffusion length is typically limited to 300 nm [4,5]. This mismatch of light absorption depth and minority diffusion length can cause insufficient absorption or carrier collection losses. As a result, efficient light management by reducing the surface reflection as well as increasing the optical path for low energy photons is important for efficiency improvements and cost reduction. Currently, quarter-wavelength transparent thin films are the industry standard for antireflection coatings (ARCs) of thin film solar cells, which are typically designed to suppress reflections at a limited spectral range and angles of incidence. In addition, light trapping is achieved by using a randomly textured Asahi U glass substrate or

#145683 - $15.00 USD Received 11 Apr 2011; accepted 14 May 2011; published 9 Jun 2011

sub-wavelength gratings on the back side [6–10]. Recently, biomimetic antireflective nanostructures have offered a new approach for suppressing the Fresnel reflection [11,12]. Due to the spatially graded structural profile in a single layer, the nanostructures not only exhibit broadband and omnidirectional antireflective characteristics, but also polarization insensitivity [13–17]. It is therefore highly desirable to incorporate such nanostructures into thin-film solar cells to simultaneously reduce the broadband surface reflection while providing optical scattering on the photon entrance front for light trapping. In this work, we demonstrate an embedded biomimetic nanostructure (EBN) incorporated into conventional p-i-n a-Si:H solar cells. The semi-oval shaped EBN exhibits antireflective and light trapping effects comparable to an industrial standard cell using an Asahi U glass substrate. Although we use a-Si:H as a test platform to demonstrate the effects of EBNs, the patterning method is broadly applicable to thin-film solar cells with other materials.

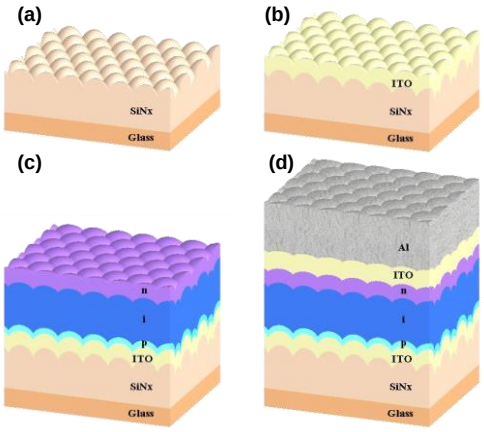

Fig. 1. The schematic fabrication flow for a-Si solar cell with an embedded biomimetic nanostructure (EBN): (a) the EBN fabricated by colloidal lithography and a reactive ion etching technique, a conformal deposition of (b) an 80 nm thick indium tin oxide (ITO) layer, (c) active a-Si:H layer (p-i-n), and (d) the aluminum back electrode.

2. Fabrication

The fabrication of EBN was done on a SiN_x layer deposited on a glass substrate using colloidal lithography followed by a reactive ion etching technique [18–24]. The choice of SiNx patterning could function as an index matching layer, while avoid potential damages resulting from patterning the frontal transparent conductive oxide. As illustrated in Fig. 1, a 380 nm thick silicon nitride (SiN_x) layer was first deposited on a glass substrate via plasma-enhanced chemical vapor deposition (PECVD). Then, polystyrene (PS) nanospheres with a plurality of 10 wt.% and diameter of 600 nm was spun-coated on the surface of the SiN_x layer, naturally arranging into a closely packed triangular lattice, which served as a self-assembled monolayer mask. Subsequently, inductively-coupled-plasma reactive ion etching (ICP-RIE) with incident oxygen (O) plasma was performed to shrink the size of PS spheres in order to facilitate the etching of SiN_x. The flow rate was set to be 20 sccm with a chamber pressure of 0.06 Pa and an RF power of 100 W. It is worth noting that the positions of PS spheres did not change during the size shrinking. The separations between PS spheres increased as their sizes decreased. Next, the ICP-RIE was performed on SiN_x and PS spheres with a CHF_3 /O_2 flow rate of 5/5 sccm, a chamber pressure of 1.33 Pa, and an RF power 150 W. The residual PS nanospheres were then removed by dipping into acetone with sonification for 5 min., as schematically shown in Fig. 1(a). Figures 1(b) to 1(d) illustrate the deposition of a single-junction a-Si:H solar cell. First, an 80 nm thick indium tin oxide (ITO) layer was deposited by DC sputtering. Then, the a-Si:H active layer with a total thickness of 292 nm (p/i/n = 12/260/20 nm) was deposited using a high-density-plasma chemical-vapor-deposition (HDP-

#145683 - $15.00 USD Received 11 Apr 2011; accepted 14 May 2011; published 9 Jun 2011

CVD) system with a growth temperate of 200°C, a constant total pressure at 900 mTorr, and a plasma power density of 0.06 W/cm^2. Finally, an 80 nm-thick indium tin oxide (ITO) layer and 500 nm of aluminum were capped on top as the back electrode and reflector. Control cells were also fabricated on a flat glass substrate with a sputtered ITO layer and a commercially available Asahi U-type glass, denoted as the flat and the Asahi U cell, respectively.

Figures 2(a) and 2(b) show the scanning electron microscopic (SEM) images of the fabricated biomimetic nanostructure and the textures of Asahi U-type glass, respectively. The EBN exhibits a periodicity of 600 nm in a hexagonal close-packed (hcp) lattice, while the Asahi U-type glass shows a randomly textured surface with uncorrelated distributions of height variations. Figure 2(c) shows a cross-sectional transmission electron microscopic (TEM) image of the fully fabricated solar cell on the EBN patterned substrate. The conformal deposition of individual layers is clearly resolved without cracks or voids that could adversely affect the device characteristics. Moreover, the inset shows a circular diffraction pattern of the corrugated p-i-n layers, which confirms the the amorphous material properties.

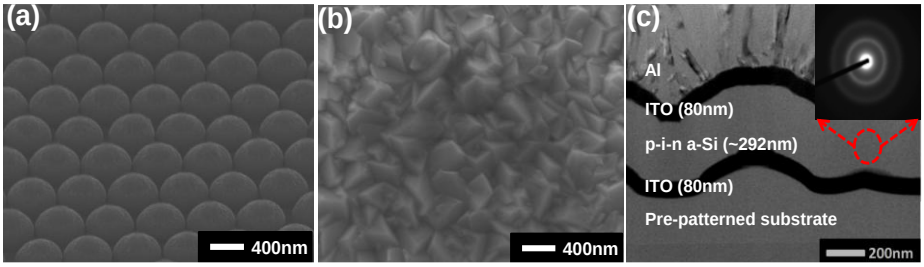

Fig. 2. Scanning electron microscopic (SEM) images of (a) the fabricated biomimetic nanostructure and (b) a commercial Asahi U substrate. (c) The cross-sectional TEM image of a fabricated solar cell on the EBN-patterned substrate. The inset shows the x-ray diffraction patterns of p-i-n layers, revealing the amorphous material properties.

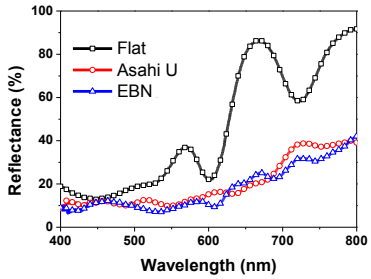

Fig. 3. The measured reflectance spectra for solar cells deposited on flat, Asahi U glass, and embedded biomimetic nanostructure (EBN) patterned substrates. The EBN and Asahi U cells reveal the enhanced absorption properties compared to the flat control.

3. Results and discussions

Figure 3 shows the reflectance spectra of fabricated cells with EBNs, Asahi U textures, and the flat substrate, which were measured with an integrating sphere at normal irradiance incidence. The reflection measurements were carried out over a broad wavelength range (400-800 nm), covering most of the solar spectrum that is absorptive to a-Si:H with a band gap of 1.75 eV (~710 nm wavelength). It can be seen that the reflectivity of cells with the Asahi U textures and EBNs are significantly lower than the flat control, reflecting the broadband absorption enhancement (A = 1-R). The reduction is particularly evident in the long wavelength range due to light trapping improvementa which increase the device absorption. Moreover, in the short wavelength range, the EBN cell shows better antireflection than the Asahi U cell. The antireflection effect arises from the tapered structural profile of the EBNs

#145683 - $15.00 USD Received 11 Apr 2011; accepted 14 May 2011; published 9 Jun 2011

which buffers the index difference between air and dielectric layers. As a result, photon transmission is enhanced for a broad spectral range, which is also reflected in the measured current-voltage (I-V) and external quantum efficiency (EQE) characteristics of the fabricated devices, as shown in Fig. 4(a) and 4(b), respectively.

The I-V measurement was performed under a simulated AM1.5G illumination condition (Oriel Class A 1000W) at room temperature following standard calibration and measurement procedures [25]. As shown in Fig. 4(a), the EBN cell shows improved short-circuit photocurrent J_{sc} = 17.74 mA/cm^2, and power conversion efficiencies η = 8.32% over the flat thin-film device (J_{sc} = 12.89 mA/cm^2 and η = 5.36%) made under otherwise identical conditions. The photocurrent and efficiency of the EBN cell is also slightly better than the Asahi U cell (J_{sc} = 17.24 mA/cm^2, η = 7.70%). On the other hand, the respective open-circuit voltage V_{oc} of the EBN and flat devices are decreased by 0.06 and 0.08 eV from 0.86 eV of the Asahi U cell. The reduction in V_{oc} results from the ITO degradation caused by high-density hydrogen plasma during the deposition of a-Si:H [26]. On the other hand, the commercial Asahi U glass substrate uses fluorine-doped tin dioxide (SnO2:F) which is rather resistive to plasmonic damage. Nevertheless, the output potential difference does not interfere with the investigation of optical improvements due to texturing, which merely impact the photocurrent. Therefore an EQE analysis was carried out to identify the origins of the photocurrent difference.

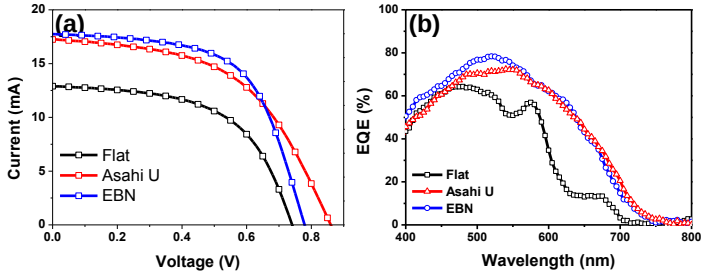

Fig. 4. (a) The current-voltage (I–V) and (b) external quantum efficiency (EQE) characteristics for solar cells deposited on various substrates: flat, Asahi U, and an embedded biomimetic nanostructure (EBN).

The EQE spectra were measured using a grating based setup with a Xenon lamp under a one-sun illumination and 0 V bias. Figure 4(b) reveals that the EBN cell exhibits a higher EQE than the Asahi U for wavelengths less than 560 nm, indicating that the photocurrent improvement mainly occurs in the short wavelength range. It is convenient to estimate a required absorption length for each wavelength component using $L = 1/\alpha(\lambda)$, where α is the absorption coefficient of a-Si:H. The calculation suggests that photons with a wavelength of λ < 620 nm can be sufficiently absorbed within the first roundtrip path, that is, L = 384 nm. Therefore light trapping is only required for λ > = 620 nm. Accordingly, the EQE enhancement before the 620 nm wavelength is attributed to the suppression of optical reflection, while the enhancement after 620 nm can result from mixed contributions of antireflection and light trapping. In the latter case, both the EBN and the Asahi U cell performs equally well for the long wavelength range. Moreover, the superior light trapping capability extends the absorption of a-Si:H to the 750 nm wavelength, beyond the estimated band edge at 710 nm. The observations are consistent with the reflectance measurement seen in Fig. 3.

Figures 5(a) and 5(b) present the calculated enhancement factors of EQE of textured cells with respect to the flat control cell for wavelengths below and above 600 nm, respectively, where the enhancement factor is defined as $\Delta EQE = EQE/EQE_{Flat}$. It can be seen in Fig. 5(a) that the antireflection property of the EBNs increases the photocurrent generation by roughly 20% for wavelengths between 400 nm and 575 nm, which is better than the Asahi U cell in this spectral range. For wavelengths longer than 575 nm, the photocurrent generation of the

#145683 - $15.00 USD Received 11 Apr 2011; accepted 14 May 2011; published 9 Jun 2011

EBN cell achieves 2 to 12-fold enhancements, compared to the control cell, shown in Fig. 5(b). The significant improvement in the infrared region indicates that the EBN can also effectively enhance the absorption by light trapping as well as the Asahi U.

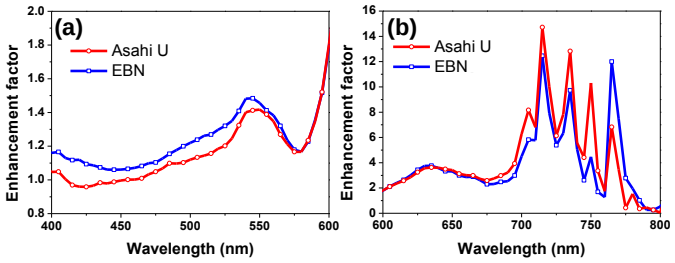

Fig. 5. The improvement factors of the EQE (ΔEQE) for EBN and Asahi U, (a) between 400 nm and 600 nm, and (b) between 600 nm and 800 nm.

4. Angular absorption

Finally, the incident-angle-dependent absorption properties are also critical to solar cells due to the sun movement. Here, we employed angle-resolved absorption spectroscopy to characterize the solar cells [27]. Figures 6(a) to 6(c) show the angular absorptive spectra for solar cells grown on flat, Asahi U, and EBN-patterned substrates, respectively. From the absorption color maps, it can be clearly seen that the EBN cell exhibits less dependency on wavelengths and incident angles than both the flat and Asahi U cells. Moreover, the high absorption region (orange-yellow, A>75%) is further extended to exceeding the 700 nm wavelength, in contrast to the cutoff at 675 nm for the Asahi U cell.

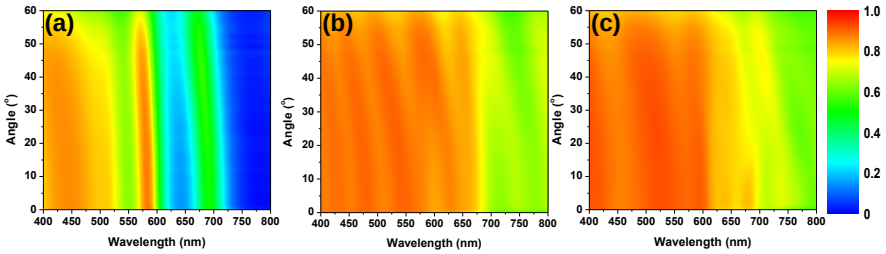

Fig. 6. The measured angular absorption spectra for solar cells deposited on (a) flat, (b) Asahi U glass, and (c) EBN-patterned substrates.

5. Conclusion

In summary, we demonstrated the superior antireflection and light trapping properties of an embedded biomimetic nanostructure incorporated into an a-Si:H thin film solar cell. The cell exhibits a higher power conversion efficiency and photocurrent than those obtainable from cells fabricated on flat and commercially available Asahi U substrates. The fabrication of the nanostructure is enabled by scalable polystyrene colloidal lithography, followed by a reactive-ion etching technique. The resulting light management effects directly enable high-efficiency a-Si:H solar cells and are also broadly applicable to other common thin film solar cells such as poly- and micro-crystalline Si, CdSe, and organic solar cells.

Acknowledgment

The authors thank the National Science Council of Taiwan for the financial support under grant number NSC99-2120-M-006-002.